

Preliminary Studies of the Obtaining of Solid Metallic Cerium from Fluoride Melts

Virgil Constantin, Ana-Maria Popescu, and Stefania Zuca

Romanian Academy, Institute of Physical Chemistry "I. G. Murgulescu",
Splaiul Independentei 202, Bucharest 77208 - Romania

Reprint requests to V. C.; Fax: +4-01-3121147; E-mail: virgilconstantin@yahoo.com

Z. Naturforsch. **58a**, 57–62 (2003); received July 28, 2001 / September 11, 2002

Presented at the NATO Advanced Study Institute, Kas, Turkey, May 4-14, 2001

The present study deals with the obtaining of solid cerium by molten salt electrolysis of a 46.74 - 48.26 - 5wt% LiF-NaF-NaCeF₄ mixture, in the temperature range 700 - 730 °C and with a current efficiency of ~75%.

For this purpose NaCeF₄ was obtained, characterized and its cubic form was identified. The solubility and decomposition potential of this compound in the molten electrolyte 49.2 - 50.8% LiF-NaF was also studied.

Key words: Cerium; Electrolysis; NaCeF₄ Decomposition Potential; Molten Salts.

1. Introduction

One of the most important rare earth metals is cerium. Molten salt electrolysis is mostly used for the winning of rare earth metals, because it allows obtaining them in a very pure state and in a few steps [1]. But until now, only liquid cerium electrodeposition was performed from halide media [2 - 4]. However on the basis of existing data, it is difficult to choose proper conditions for the electrolysis of cerium compounds.

Most details concerning the preparation of cerium metal are manufacturing secrets. Taking in account that Zr, Hf, Ta, and Nb can be obtained by electrolysis of their compounds: K₂ZrF₆, K₂HfF₇, K₂TaF₇, and K₂NbF₆, we assumed that also Ce can be obtained from one of its compounds.

From all the compounds formed by CeF₃ with the alkali fluorides [5, 6] we selected NaCeF₄ because it is easily synthesized and is not hygroscopic as the compounds formed with K. However there are no literature data about the structure and electrochemical behaviour of NaCeF₄.

The present study deals with the winning and characterization of NaCeF₄, followed by the determination of its solubility and decomposition potential in the electrolysis bath. Finally, solid cerium was electrodeposited by decomposition of the compound and the current efficiency of the process was determined.

2. Experimental

P. a. grade Merck and Fluka NaF and CeF₃ were placed in quartz cells and heated at 400 °C under vacuum to remove any moisture. Then the salts were carefully mixed and transferred to the electrolysis cell. The system was maintained under vacuum or in a dry argon atmosphere.

In Fig. 1 the assembly for the experimental work is presented. The water-cooled working cell (Fig. 2) was built entirely of stainless steel.

The electrolytic bath was a mixture of LiF and NaF (61 and 39 mol%) with a varying content of NaCeF₄.

The electrolysis was performed at 700 - 740 °C, using a cylindrical spectral graphite anode (ϕ = 5 mm) and a molybdenum cathode (ϕ = 2mm) of 99.95% purity, produced by Johnson-Matthey. The molybdenum cathode was tightly fastened in a BN sheath in order to define accurately the surface area. The reference electrode was a Pt wire.

For obtaining NaCeF₄, the individual fluorides were mixed in equimolar proportions and then melted in a crucible inside the electrolysis cell at 745 °C. Finally the crucible was fast-cooled by ice quenching.

DTA, IR-spectroscopy and XRD measurements were carried out for the characterization of the NaCeF₄ compound obtained in this way.

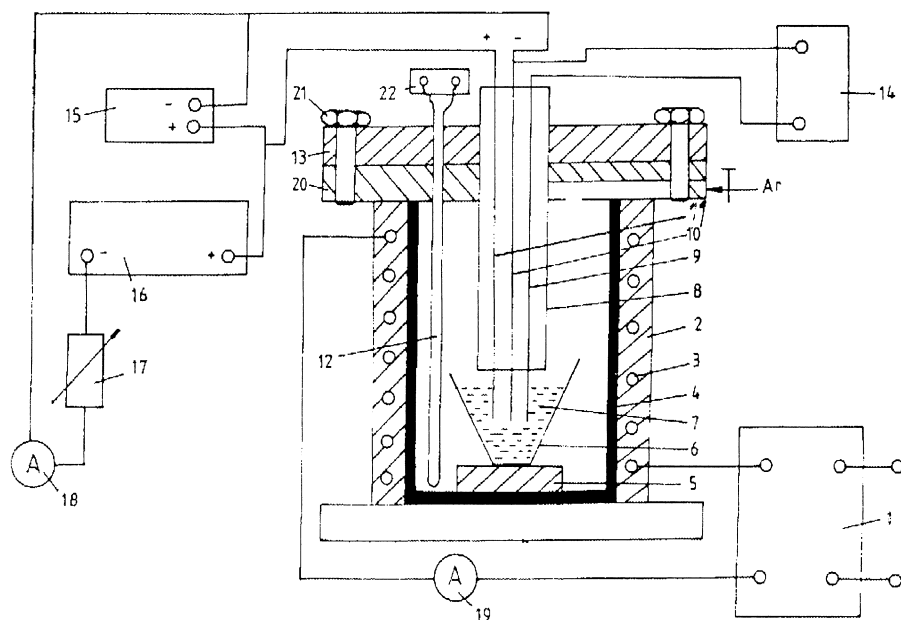


Fig. 1. The assembly for the experimental work. 1. Autotransformer; 2. Furnace; 3. Furnace electric resistor; 4. Electrolytic cell; 5. Crucible support; 6. Pt crucible; 7. Electrolyte; 8. Electrodes sheath; 9. Reference electrode; 10. Cathode; 11. Anode; 12. Sheath + thermocouple; 13, 20. Flanges; 14, 15, 22. Digital multimeters; 16. D. C. source; 17. Adjustable resistance; 18, 19. Amperimeter; 21. Flange screw binding.

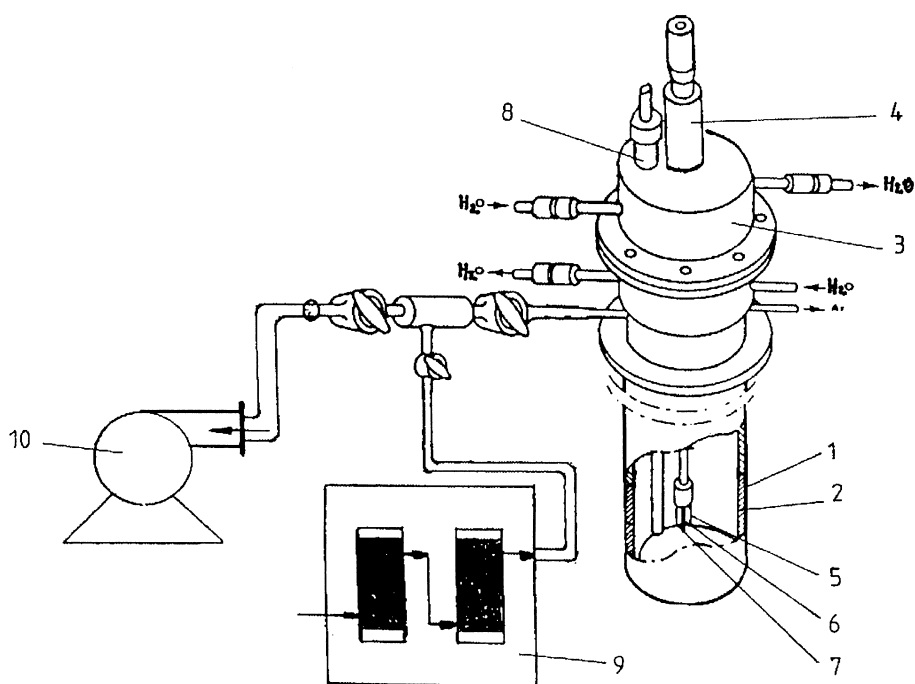


Fig. 2. The water-cooled working cell 1. Stainless steel retort; 2. Pt crucible; 3. Water cooled upper part; 4. Support of electrodes; 5. Graphite anode; 6. Mo cathode; 7. Pt reference electrode; 8. Pt-Pt/Rh thermocouple; 9. Ar purification line; 10. Vacuum pump.

An OD-103 MOM-Budapest derivatograph was used to record the differential thermal effects, with α -Al₂O₃ as reference.

IR spectra were recorded on KBr, using an M-80 / SPECORD-Carl Zeiss Jena type spectrometer. Samples for IR characterization were pressed as pellets and made from homogenous mechanical mixtures of 0.5 mg NaCeF₄ and 200 mg KBr.

Diffraction measurements were carried out with a DRON-3 diffractometer of 2 θ type reflection geometry, using a copper lamp with a nickel monochromator (CuK α = 1.5418Å).

The solubility of NaCeF₄ in the electrolytic bath was investigated by visual observation, and the decomposition tension was determined using the potential-current curves method with increasing and decreasing current steps.

3. Results and Discussions

The NaF-CeF₃ binary system [5 - 7] exhibits the NaCeF₄ 1:1 compound.

The phase diagram for this system was reported by R. E. Thoma [8]. It exhibits an eutectic at 726 °C, and the NaCeF₄ stoichiometry has a limited stability range since it decomposes peritectically at 810 °C.

DTA, IR-spectroscopy and X-ray diffraction were used for the characterization of the NaCeF₄ compound.

The DTA thermogram exhibits 2 peaks (Fig. 3). The first one, very sharp, starts at 726 °C while the second one starts at the end of the first effect, i. e. around 810 °C. This second peak has a typical shape [9] and corresponds closely to the peritectic decomposition temperature observed by Thoma [8].

The further contribution observed on this same peak may be due to CeO₂ impurity. The temperature 726 °C of the first peak, that corresponds to the formation of NaCeF₄ is also in excellent agreement with Thoma [8].

As nothing is known about the structural features of NaCeF₄ this compound was investigated by IR spectroscopy together with CeF₃ for of comparison (Fig. 4).

We observed first that the two well-marked peaks of CeF₃ transform into a broad peak of NaCeF₄. However, the first peak at 380 cm⁻¹ in CeF₃ may correspond to the shoulder at 390 cm⁻¹ in NaCeF₄, while the second one around 250 cm⁻¹ is shifted to 260 cm⁻¹. These differences can be ascribed to the

formation of NaCeF₄. In addition, the disappearance of the peak at 380 cm⁻¹ to a shoulder can be ascribed not only to the formation of NaCeF₄, but also to the change of the coordination polyhedron of Ce³⁺ (in the passing) from CeF₃ to NaCeF₄.

The XRD pattern obtained for NaCeF₄ at room temperature (Fig. 5) shows that, in addition to the features of NaF and CeF₃, there is also a new line that characterizes the NaCeF₄ compound.

We also observed that it occurs very close to the line corresponding to CeO₂, that is also present in the pattern which indicates the presence of a small oxide amount as an impurity. This amount was determined as about 3%. Comparing those results with literature data [10 - 13], and by comparison with the NaPrF₄ compound with cubic symmetry, a complete single-crystal structure analysis has been carried out to establish the details of the NaCeF₄ structure. We found that NaCeF₄ is cubic at room temperature. The lattice parameter of the elemental cell was found as $a_0 = 5.328 \text{ \AA}$, thus similar to that of NaPrF₄ ($a_0 = 5.320 \text{ \AA}$), which was predictable as the atoms of Ce and Pr differ only by one electron on the level 4f.

We expect the small oxide impurities to have a minor influence on the electrolytic process.

In order to establish the optimal composition of the electrolytic bath we studied the solubility of NaCeF₄ in the LiF-NaF (49.2 - 50.8 wt %) melt. From the change of the solubility with temperature in the range 700 - 800 °C we assumed that the optimal composition range for using that compound for the electrodeposition of cerium is 5 - 10%.

Figures 6 and 7 present the current-potential curves in the systems LiF-NaF-5%NaCeF₄ and LiF-NaF-10%NaCeF₄ at 730 °C. The resistance of the electrolyte was measured with a Wayne-Kerr bridge (with a 0.1% precision) and was found to be 0.28 Ω .

Starting from the relation

$$E = U - IR,$$

where E [V] is the counter electromotive force, U [V] the cell voltage, I [A] the current intensity, and R [Ω] the cell resistance.

The I - U curves were transformed to I - E curves, and from the extrapolation to zero current of the linear part of those plots the decomposition potential (E_{dec}) was evaluated.

The mean value of the decomposition potential, was found to be $E_{\text{dec}} = 2.025 \text{ V}$, and it does not vary with the concentration of NaCeF₄.

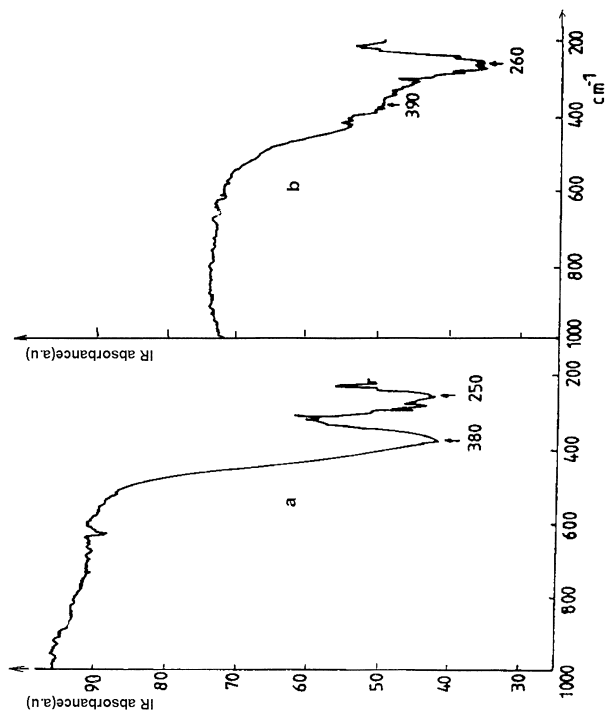


Fig. 4. IR spectrum of CeF₃ (a) and NaCeF₄ (b).

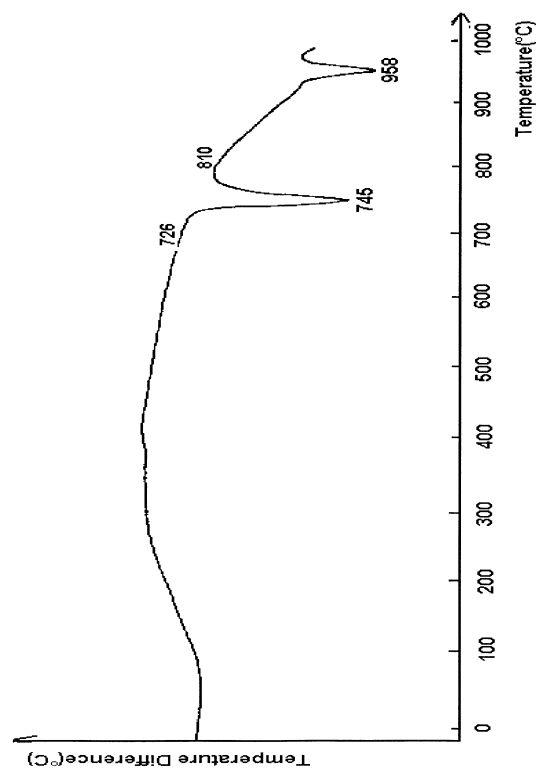


Fig. 3. DTA thermogram of NaF-CeF₃ (50 - 50 mol%).

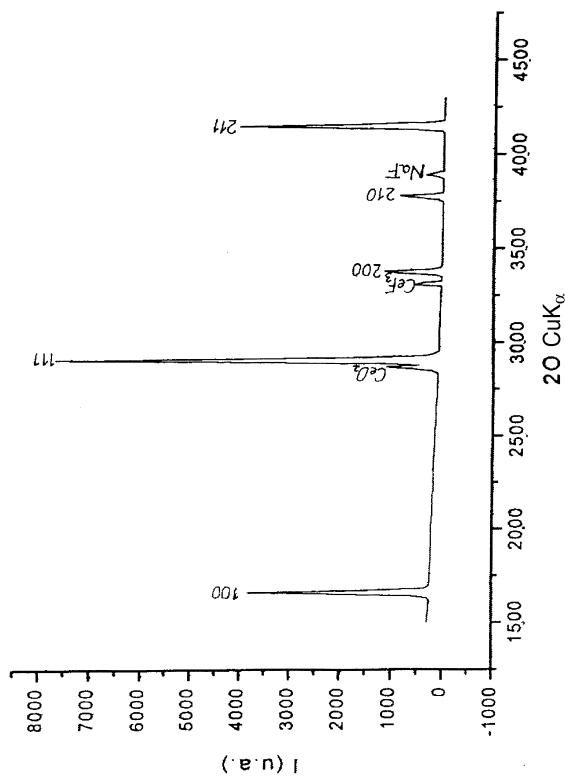


Fig. 5. X-ray diffraction pattern of NaCeF₄.

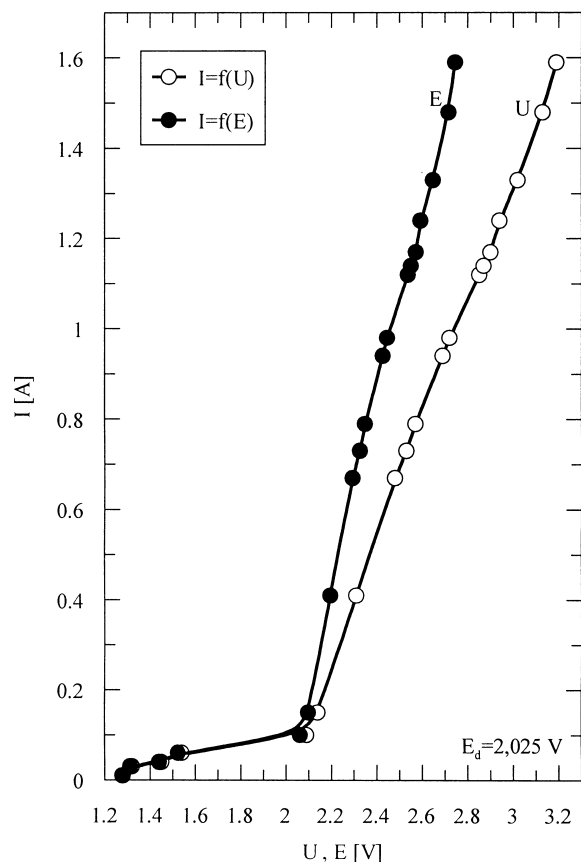


Fig. 6. Current-potential curves of the system LiF - NaF - 5%NaCeF₄ at 730 °C.

The value found for the decomposition potential of NaCeF₄ demonstrates that Ce will be deposited before Li and Na, as their decomposition potentials are larger ($E_{\text{dec}}^{\text{LiF}} = 5.358 \text{ V}$, $E_{\text{dec}}^{\text{NaF}} = 4.917 \text{ V}$).

At the end of this study we performed the electrolysis of the LiF-NaF-NaCeF₄ (46.74 - 48.26 - 5 wt%) under the following conditions: temperature 730 - 750 °C, current density 2.5 Acm⁻², potential 5.5 - 6 V, time 1 - 2 h, distance anode-cathode = 2 mm, surface of the anode 0.1963 cm² and surface of the cathode 0.0314 cm².

Several electrolyses (3 - 8) were carried out under the same conditions and the reproducibility of the cerium deposit was very good. A thin deposit of solid metallic cerium of 99.5% purity (determined by XRD measurements) was obtained with a current efficiency

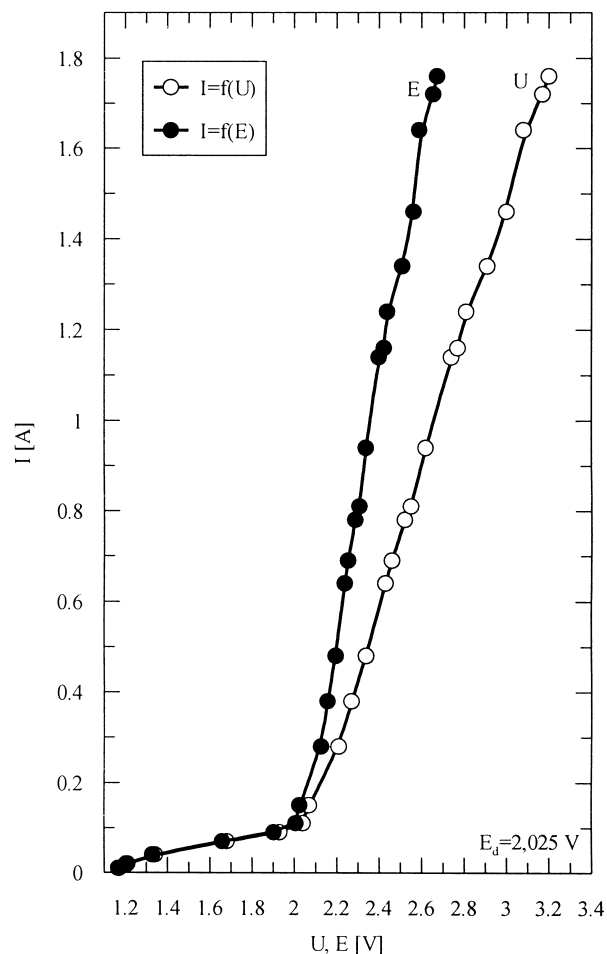


Fig. 7. Current-potential curves in the system LiF - NaF - 10%NaCeF₄ at 730 °C.

of ~75% (calculated by measuring the total amount of the cathodic deposit).

4. Conclusions

For the first time the existence of cubic NaCeF₄ was observed.

It was demonstrated that it is possible to obtain solid metallic cerium by electrodeposition from molten LiF-NaF-NaCeF₄.

However, the utilization of this method requires some systematic electrode process-, current efficiency- and granulometric studies.

- [1] T. A. Restivo and E. J. Pessine, *Science Forum* **73-75**, 533 (1991).
- [2] A. Bogacz, L. Rycerz, S. Rumianowski, W. Szymanski, and W. Szklarski, in "Advances in Molten Salts - From Structural Aspects To Waste Processing", Proceedings of the European Research Conference on Molten Salts, Porquerolles Island, France, 1998, ed. Marcelle Gaune-Escard, Begell House, Inc. 1999, 526.
- [3] N. Ene and S. Zuca, *Rev. Roum. Chim.* **43**, 817 (1988).
- [4] V. Soare, PhD-Thesis, Bucharest 1997.
- [5] V. Constantin and A. M. Popescu, *Rev. Chim.* **51**, 751 (2000).
- [6] A. M. Popescu, V. Constantin, and R. Birjega, *Rev. Chim.* **51**, 428 (2000).
- [7] V. Constantin, I. Gherghescu, A. M. Popescu, and R. Birjega, *Sci. Bull. UPB, Serie B*, **60**, 177 (1998).
- [8] R. E. Thoma, H. Insley, and M. Herbert, *Inorg. Chem.* **5**, 1222 (1966).
- [9] M. Gaune-Escard, in "Molten Salts: From Fundamentals to Applications", Proceedings of the NATO Advanced Study Institute on Molten Salts 2001, ed. Marcelle Gaune-Escard, NATO Science Series, Series II: Mathematics, Physics and Chemistry, Kluwer Academic Pub. **52**, 401 (2001).
- [10] R. E. Thoma, G. M. Herbert, H. Insley, and F. Weaver, *Inorg. Chem.* **2**, 1005 (1963).
- [11] R. E. Thoma, C. F. Weaver, H. A. Friedman, H. Insley, L. A. Harris, and H. A. Jakel, *J. Phys. Chem.* **65**, 1096 (1961).
- [12] D. M. Roy and R. Roy, *J. Electrochem. Soc.* **111**, 421 (1964).
- [13] ASTM-X Ray Diffraction, Card Nr: 8-45, 6-0325, 12-788, 10-123, 25-817, 22-1393.